

Influence of supercritical debinding and processing parameters on final properties of injection-moulded Inconel 718

Alexandre Royer^{1a}

alexandre.royer@femto-st.fr

Thierry Barriere^{1a}*

thierry.barriere@univ-fcomte.fr

Yves Bienvenu^{2b}

yves.bienvenu@mines-paristech.fr

^{1a}Univ. Bourgogne Franche-Comté, FEMTO-ST Institute, CNRS/UFC/ENSMM/UTBM, Department of Applied Mechanics, 25000 Besançon, France

^{2b}Mines Paris Tech, Centre des Matériaux, UMR CNRS 7633, Evry, France

*Corresponding author.

Abstract

In the metal injection-moulding process, the thermoplastic polymer binder plays an essential role as it provides fluidity to the high-loaded feedstock and strength to maintain the moulded shape. The purpose of this study is to develop an environmentally friendly feedstock loaded with a super-alloy Inconel 718 powder. Different binder formulations based on polyethylene glycol (PEG), for its water solubility, and bio-sourced polymers were investigated. Poly(lactic acid)/poly(hydroxybutyrate-valerate) was investigated as a bio-sourced polymer because its miscibility with the PEG. The results are compared to a standard formulation using polypropylene and PEG developed by our research group. A micro powder of Inconel 718 (nickel-based super-alloy) was chosen to elaborate the feedstock. The chemical and rheological behaviour of the feedstock during the mixing, injection, and debinding processes were investigated, with tight control of each process. The comparative impacts of the two different debinding processes and optimum sintering parameters were investigated: one by water and one by CO₂ in supercritical state. The supercritical debinding caused no damage to the components for all types of feedstock and decreased the time to remove the PEG from 48 h to 4 h. Finally, the density, microstructure, and hardness of the different samples after final heat treatment were compared. The microstructure was clearly optimized, as the γ phases were promoted inside the grains. The results show that the well-adapted binder and debinding process produces an Inconel 718 component with high mechanical properties (Vickers hardness of 341 ± 19 HV). Moreover, this approach can be used with other formulations, powders, and binder systems.

Keywords: Metal injection-moulding; Inconel 718; Supercritical debinding; Bio-sourced polymers; Grain size effects

1.1 Introduction

Metal injection-moulding (MIM) is a process to produce a small-mass component with complex geometry from varied materials such as stainless steel and superalloys. This process is based on the injection of a feedstock composed of the powder of a desired material required for the final component, and a thermoplastic binder composed of several polymers. After injection-moulding, the binder is removed from the component using a solvent and then by heating. The component becomes a porous metal skeleton which is finally sintered to obtain the final dense functional component with mechanical properties similar to those of a wrought material. The binder has the multitasking role of being able to support an important powder-loading rate in volume, typically 60%, to carry the powder into the mould die cavity [1,2] and be easily removable. To satisfy these properties, binders are generally composed of three components [1]: one to provide the necessary fluidity (flux), one to provide strength to the injected component (backbone), and one to act as a surfactant to prevent the aggregation of the powder particles [1,3,4].

Currently, binders are composed of petroleum-sourced polymers and require hazardous solvents to be removed. The formulation developed previously at our laboratory is composed of polypropylene for the backbone, paraffin wax as the flux, and stearic acid as the surfactant [5,6]. This binder needs cyclohexane as a solvent, which is a poisonous chemical. Some new green formulations were developed in previous studies [7–9], and the main goal of this study was to determine the effect of the formulation and debinding process on the properties of the final component. First, to avoid chemical solvents, polyethylene glycol (PEG) was chosen as the flux because it is water soluble. PEG contains terminal hydroxyl groups which provide water solubility for molecular masses ranging from 400 to 40,000 g·mol⁻¹ [10–12]. Therefore, PEG with a molecular weight of 20,000 g·mol⁻¹ was chosen as it ensures solubility in water while maintaining a sufficient binder viscosity. Backbone bio-sourced polymers were chosen to reduce the environmental impact because the backbone is removed by heating. Polylactic acid (PLA) and poly(hydroxyacanoate) (PHA) were chosen because there are the most common bio-sourced polymers used in the injection-moulding industry. PLA and PHA are biodegradable and biocompatible polymers with good physical, mechanical, and thermal properties [10,13]. PLA is obtained from the polycondensation of lactic acid which is produced by bacterial fermentation of corn starch or cane sugar. PHA is a polyester obtained directly from the bacterial metabolism. Under conditions of

limiting nutrients and in the presence of an excess carbon source, bacteria synthesizes PHA granules in the size 0.2–0.5 μm [13]. Stearic acid was used as the surfactant [14].

The first step of the debinding process consists of removing the plasticizer binder from the component by using a solvent. This process is time-consuming and creates defects which affect the properties of the sintered components [1,3]. Moreover, the traditional solvents are hazardous. The use of a fluid in a supercritical state as a solvent permits the reduction of the debinding time, to produce defect-free components and the use of a green and sustainable extraction process. This process was first used by Chartier et al. [15] on ceramic powder, and Shimizu et al. [16] applied it on metallic powder. It consists of placing the component in an enclosure subjected to pressure and temperatures higher than the critical point to perform polymer extraction. This method is based on the transport properties and solvent power of supercritical fluids which are better than those of other organic solvents. CO_2 is the most commonly used supercritical solvent fluid because of its low cost, non-toxicity, inflammability and capacity to extract organic compounds with low molecular mass [17].

The material chosen as the powder was Inconel 718, a nickel-based superalloy. Inconel was developed to meet the needs of complex aeronautic engines, where mechanical and thermal solicitations are colluding at high levels for long periods [18]. So Inconel is used in aviation, aerospace, and nuclear power applications because of its high resistance to corrosion and oxidation and also for its excellent mechanical strength at high temperatures [19–21]. Inconel is a family of approximately 25 superalloys composed of nickel and chromium. The high nickel content significantly increases its elasticity limit and yield stress [22]. The chromium content is strengthens its the oxidation resistance and the niobium content is responsible for the formation of the hardening phase γ'' [23], and increases the hardness and elasticity limit of Inconel. Inconel 718 contains the maximum allowable concentration of niobium for this kind of alloy because the higher niobium concentration, the more it is increased until a limit around 5% mass. Titanium and aluminium are elements responsible for the formation of the γ' phase [24], the hardness of the structure, and to a lesser degree the γ'' .

The use of Inconel for the MIM process has been studied by Özgün et al. [19,20] and Valencia et al. [25]. The binders developed by Özgün et al. [19,20] were conventional formulations composed of polypropylene (PP), carnauba wax, paraffin wax and stearic acid. The powder used in this process was a micro-sized spherical powder. This powder was used to facilitate the injection-moulding of small components, the sintering was faster, and the final mechanical properties were improved better [26].

The main goal of the present study was to develop an environmentally friendly binder formulation adapted to the use of a micro-sized Inconel 718 powder. Three studies were performed. The first chose and validate the bio-sourced polymer subject to high mechanical and thermal stress used for the elaboration of the binder and functional components. The second developed and optimized the use of the CO_2 in a supercritical state as a solvent of the PEG. The final study sintered the component and validated the final mechanical properties in terms of hardness with, tight control of each process step.

2.2 Materials and methods

The polymers used in this study were polypropylene, poly(3-hydroxybutyrate-co-3-hydroxyvalerate) (PHBV), and PLA as the backbone binder, PEG as the plasticizer, and stearic acid as the surfactant. Two kinds of PLA were tested, PLA005 and PLA003. The PLAs were supplied by Nature Plast (France), the PP, PEG, and the stearic acid by VWR (France), and the PHBV by L. Hilliou from IPC/I3N, Guimarães (Portugal).

The metal powder used was a gas-atomized powder of Inconel 718 provided by Sandvik Ospreys (England) with spherically shape grains with a median diameter of 8.7 μm . Figure 1 shows an optical microscopy image of the polish powder to view the internal porosity of the particles. On this micrograph, no internal porosity was observed.

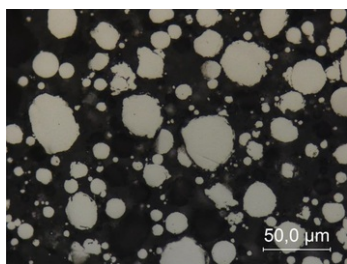


Figure 1 Fig. 1 Optical microscopy of micro-sized Inconel 718 powder.

alt-text: Fig. 1

The feedstocks were elaborated in a twin-screw mixer (Brabender Plastograph®, Germany). The powder and binder were mixed at 50 rpm and 170 °C. The composition of the different feedstocks is given in Table 1. The components were formed on a hydraulic horizontal injection-moulding press (Arburg®, Germany) at 170 °C and 100 MPa. The injected cylindrical specimens were 35-mm long with a diameter of 10 mm. The weights of the injected specimens had a mean deviation of 0.05 g, showing good homogeneity of the elaborate components. To perform the water debinding, the specimens were placed in a batch of heat-stirred water [27,28]. Two different temperatures were studied, 50 °C and 60 °C, and the tests lasted during 24 h and 48 h. The samples were then dried in a furnace at 50 °C for 4 h. The samples were weight dried before and after the debinding process to determine the quantity of PEG removed.

Table 1 Composition of different feedstocks studied with same Inconel 718 powder.

alt-text: Table 1

Formulation	Powder loading rate % vol.	Primary binder % vol.	PEG % vol.	Stearic acid % vol.
1	60	16 of PP	22	2
2	60	16 of PLA005	22	2
3	60	16 of PLA003	22	2
4	60	16 of PHBV	22	2

The supercritical debinding process was carried out with a supercritical reactor provided by Separex©. The same method of drying and weighing was applied to the samples debinded by CO₂. According to previous works [7], the supercritical debinding tests were performed at 40 MPa of CO₂ pressure. Three different temperatures (70 °C, 120 °C, and 150 °C) were tested on different formulations.

The thermal debinding and sintering of the debinded components were realized by the same process. The part was heated at 2 °C/min to the thermal debinding temperature and maintained at this temperature for 1 h; the thermal debinding temperature depends on the formulation. Table 2 lists the thermal debinding temperature for all formulations. Then the sample was heated at 5 °C/min to 1290 °C and maintained at this temperature for 3 h. The cooling was realized at 20 °C/min. The thermal debinding and sintering were performed under an argon atmosphere. The sintering process was optimized from the Özgün et al. work [20]. The test samples and conditions of the tests are available in Table 3.

Table 2 Temperature of thermal debinding for different feedstocks.

alt-text: Table 2

Formulation	1	2	3	4
Temperature of thermal debinding	325 °C	290 °C	250 °C	235 °C

Table 3 Density and Vickers hardness of components versus debinding method after sintering.

alt-text: Table 3

Sample	A	B	C	D	E
Formulation	1	3	4	1	2
Debinding method	Water	Water	Water	CO ₂	CO ₂
	60 °C, 48 h	60 °C, 48 h	60 °C, 48 h	150 °C, 4 h	80 °C, 8 h
Density (%)	98.7	94.0	99.7	95.9	95.2
Hardness (HV)	268 ± 5	212 ± 26	259 ± 9	198 ± 18	204 ± 13

The density of the samples was determined using a helium pycnometer. An optical microscopy and SEM analysis were also performed.

3.3 Results

3.1.3.1 Water and supercritical debinding

PEG was chosen because of its ability to be removed by water. Figure 2 shows the quantity of PEG removed versus time at different temperatures for Formulation 1. The speed of PEG removal is temperature dependant; therefore, 60 °C, which is close to the melting temperature of PEG, was chosen. The result for the Formulation 4 was similar. Formulation 2 could not be debinded because the component disappeared totally during the water debinding process. This is probably because of the interaction between PLA and PEG during mixing [29] which changes the crystallinity of PLA and enhances its degradation. Formulation 3 caused huge cracks and defects in the sample and could not be debinded by water. The differences in behaviour between Formulations 2 and 3 is owing to the difference in the percentage of PLLA in the two PLAs which changes the crystallinity of the two polymers. Figure 3 shows images of the components before and after water debinding. The results show no defects after 48 h in 60 °C water for Formulations 1 and 4.

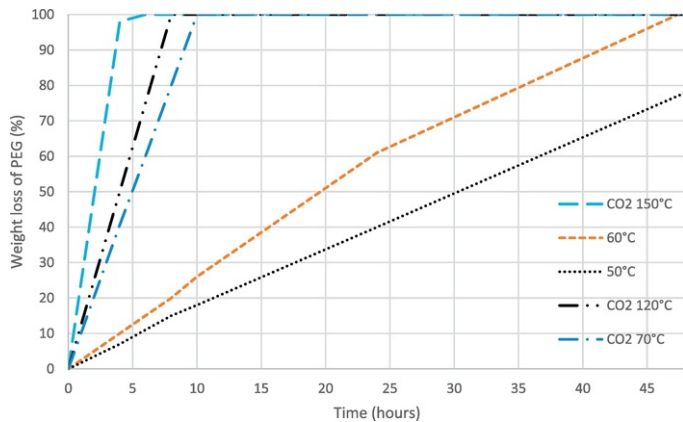


Figure 2 Fig. 2 Evolution of weight loss of PEG versus time during water debinding and supercritical debinding processes.

alt-text: Fig. 2



Figure 3 Fig. 3 Images of components before and after water debinding for Formulations 1, 3, and 4.

alt-text: Fig. 3

According to the results of the water debinding process, 48 h is the time required to remove 100% of the PEG from a component at 60 °C. To reduce this time, CO₂ in a supercritical state was used as the solvent. The result of the supercritical debinding of Formulation 1 is shown in Figure 2. The time of debinding was reduced by increasing the temperature. The time to remove 100% of the PEG was reduced by 480% at 70 °C, 800% at 120 °C, and 1200% at 150 °C. The components can be debinded at higher temperatures during supercritical debinding instead of temperatures lower than the PEG melting temperature in water debinding without defects. Figure 4 shows pictures of samples of the different formulations after supercritical debinding. All formulations were debinded by CO₂ in a supercritical state without defects.



Figure 4 Fig. 4 Images of components versus associated formulations after supercritical debinding at 70 °C during 4 h for Formulations 1–4.

alt-text: Fig. 4

3.2.3.2 Thermal debinding and sintering

The shrinkage of the samples during sintering was measured by a dilatometer and the result is shown in Figure 5. These results show a larger shrinkage for the sample debinded by a supercritical fluid. A significant shrinkage normally means a better sample density. To validate this result, the density measurement was performed by helium pycnometry. The result given in Table 3 shows better component density debinding by water. However, the component of Formulation 3 debinded by water had the lowest density. The Formulation 2 sample debinded by supercritical CO₂ also had lower density than that of the Formulation 1 sample debinded by the same process because the PLA in the binder of this formulation which was unadapted to the MIM process.

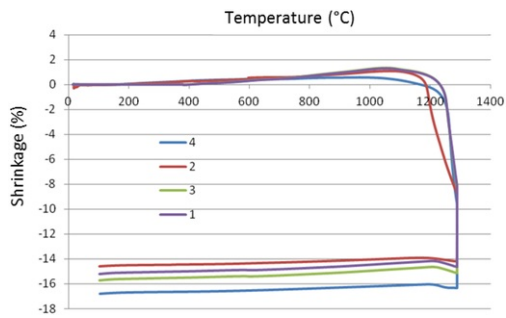


Figure 5 Fig. 5 Shrinkage curve evolutions of different components during the sintering process with Formulations 1-4.

alt-text: Fig. 5

3.3.3.3 Hardness characterization

The hardness of the samples was determined using the Vickers method. The tests were performed 10 times on each samples using 0.1 HV of normal stress. The results are given in Table 3. The standard deviation provides an indication of the homogeneity of the sample. Theoretically, the Vickers hardness of the Inconel 718 after sintering is 250 HV [22]. Samples B, D, and E had low hardness and a significant standard deviation because of the high porosity rate in these samples probably caused by the debinding process and/or the feedstock. Samples A and C exhibit an expected Vickers hardness.

3.4.3.4 SEM analysis

SEM images of the different samples were obtained and energy-dispersive X-ray spectroscopy analysis was performed to determine possible pollution and the distribution of the elements. Figure 6 shows the microscopies. These results show pores according to the density results. The energy-dispersive X-ray spectroscopy analysis focused on: titanium, niobium and aluminium, which are the constitutive elements of precipitation hardening in Inconel 718 [23,30]. This precipitation hardening results from the appearance of the γ_2' and γ_2'' phases [23]. The γ_2' and γ_2'' are composed of $\text{Ni}_3(\text{Ti,Al})$ and Ni_3Nb , respectively [31]. Titanium and niobium can produce $\text{C}(\text{Ti,Nb})$ carbide which precipitates at the grain boundary and prevents the formation of the γ_2' and γ_2'' phases. They also can create defects at the grain boundary [32]. The distribution of the elements of the γ_2' and γ_2'' phases in the different samples is shown in Figure 7. This figure shows significant concentrations of niobium, titanium, and aluminium around the porosity. In accordance with Figure 6, Figure 7 shows some defects where niobium, titanium and aluminium are present. However, the carbon distribution shows that carbon is present with niobium and titanium, meaning that the presence of niobium and titanium corresponds to carbide $\text{C}(\text{Ti,Nb})$. Carbon can be produced during the burning of the polymers and enhances the precipitation of carbides [33].

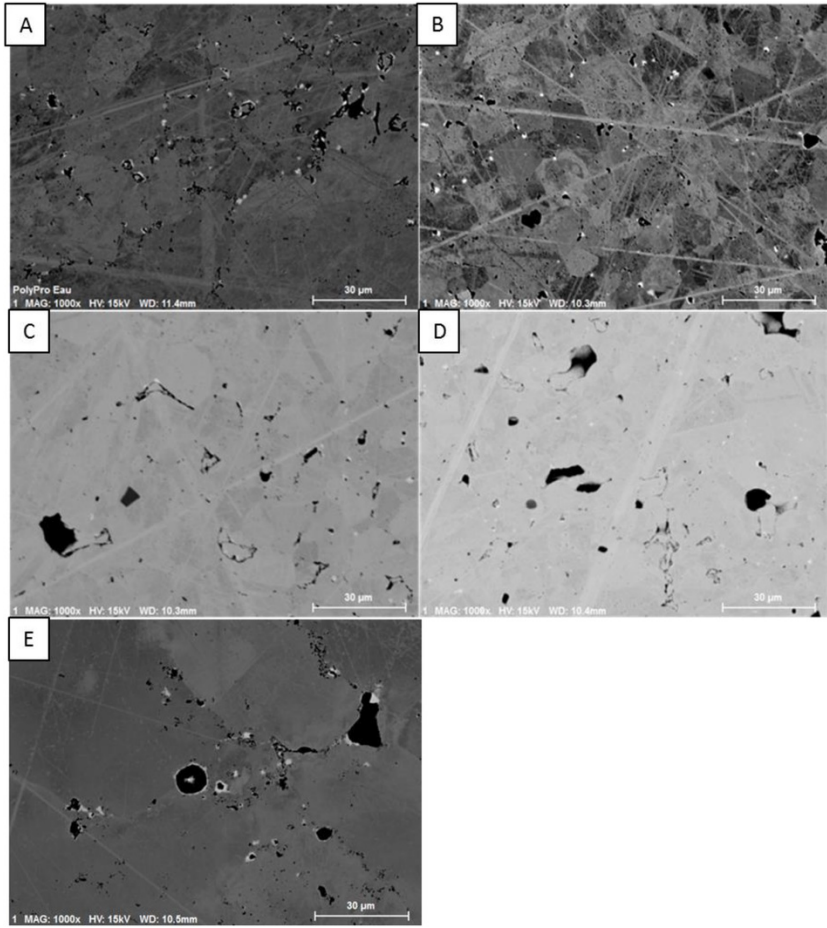


Figure 6 SEM images of Samples A, B, C, D, and E.

alt-text: Fig. 6

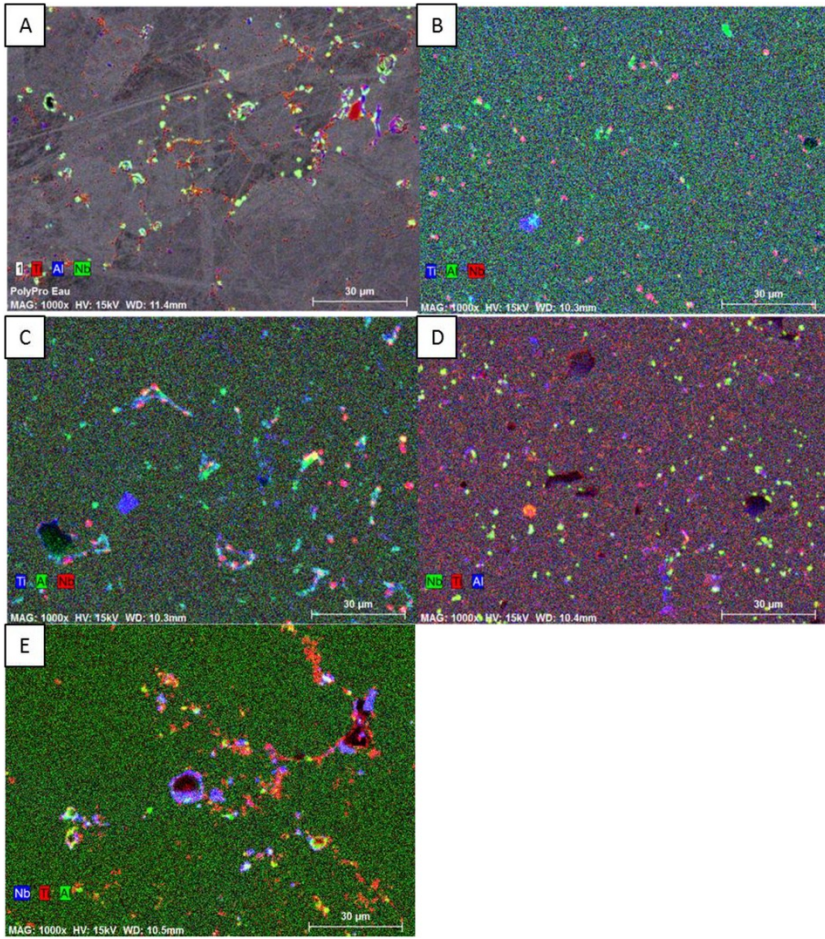


Figure 7 Fig. 7 SEM images with energy-dispersive X-ray spectroscopy analysis of Samples A, B, C, D, and, E.

alt-text: Fig. 7

Moreover, some grey precipitates, as seen in Figure 8, are composed of titanium and nitrogen. These precipitates correspond to the formation of titanium nitride. The nitrogen presence can result from a poor vacuum quality in the sintering atmosphere.

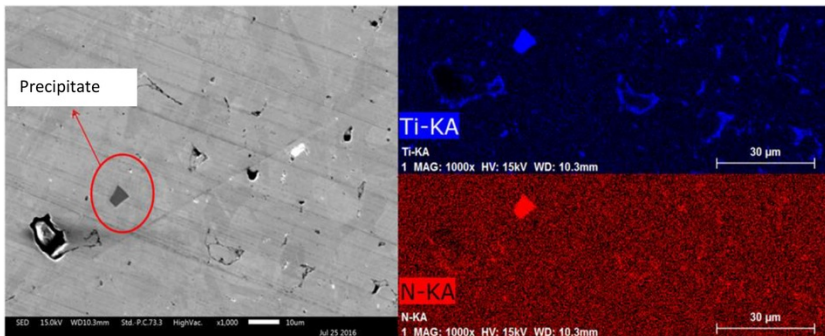


Figure-8 Fig. 8 SEM images with energy-dispersive X-ray spectroscopy analysis of Sample C.

alt-text: Fig. 8

To improve the mechanical properties of the final component, a heat treatment was performed by heating the sintered sample to 750 °C for 1 h, followed by a cooling rate of 100 °C/min. This heat treatment enhanced the precipitation of the γ_2' and γ_2'' phases and improved the hardness [34]. This post treatment was performed on sample A. The results show a Vickers hardness of 341 ± 19 HV, an even lower density than that of the sample tested (97.6%). This density value was probably the result of the debinding or injection process. The sample of Figure 9 shows an increase in the grain size to 15 μ m.

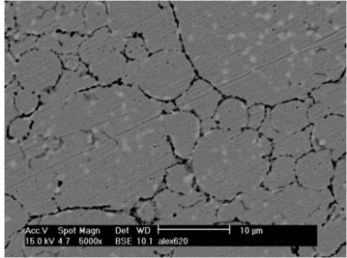


Figure-9 Fig. 9 SEM image of Sample A after heat treatment.

alt-text: Fig. 9

4.4 Conclusion

Comparative impact of two different debinding processes and optimum sintering parameters was investigated with dedicated new formulations based on environmentally friendly polymers and Inconel superalloy powders for MIM applications.

The results show that PLA005 is not adapted to water debinding and the use of the PLA/PHA/PHBV polymers as primary binders causes cracks during water debinding and increases the time to totally remove the PEG. The supercritical debinding caused no component damage for all types of feedstocks and decreased the PEG removal time from 48 h to 4 h. The components made with the PLA binder exhibited the lowest density and hardness. The same results were found for the samples debinded by the supercritical debinding process.

The density, microstructure, and hardness of the samples after the heat treatment were also compared. The microstructure was clearly optimized because, the γ_2' phases were promoted inside the grains. The results show that the well-adapted binder, associated the debinding process, and process parameters were successful in obtaining MIM components without defects and with high mechanical properties (Vickers hardness of 341 ± 19 HV).

The procedures and associated processing parameters proposed in this study represent the overall experimental data and physical analysis; therefore, they can be readily employed in other formulations, powders, and binder systems using the powder injection-moulding process.

Acknowledgement

The authors wish to thank the FUI ProPIM project for its financial support, Sophie Lamy of Alliance MIM company for the MEB analysis and Loic Hilliou from IPC/I3N, Guimarães, Portugal for the PHBV.

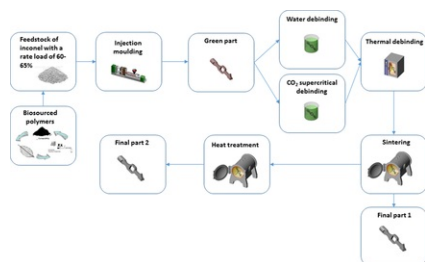
References

- [1] R.K. Enneti, V.P. Onbattuvelli and S.V. Atre, 4 - Powder binder formulation and compound manufacture in metal injection molding (MIM), In: D.F. Heaney, (Ed), *Handbook of Metal Injection Molding*, 2012, Woodhead Publishing, 64–92
<http://www.sciencedirect.com/science/article/pii/B9780857090669500042>, Accessed 12 June 2015.
- [2] M.R. Raza, A.B. Sulong, N. Muhamad, M.N. Akhtar and J. Rajabi, Effects of binder system and processing parameters on formability of porous Ti/HA composite through powder injection molding, *Materials & Design Mater. Des.* **87**, 2015, 386–392,
<https://doi.org/10.1016/j.matdes.2015.08.031>.
- [3] R.M. German, *Powder Injection Moulding - Design and Applications*, 2003, Innovative Material Solution, Inc..
- [4] Y. Li, X. Liu, F. Luo and J. Yue, Effects of surfactant on properties of MIM feedstock, *Transactions of Nonferrous Metals Society of China. Trans. Nonferrous Metals Soc. China* **17**, 2007, 1–8, [https://doi.org/10.1016/S1003-6326\(07\)60039-9](https://doi.org/10.1016/S1003-6326(07)60039-9).

- [5] J. Bricout, P. Matheron, C. Abitzer, J.C. Gelin, M. Brothier and T. Barrière, Evaluation of the feasibility of the powder injection moulding process for the fabrication of nuclear fuel and comparison of several formulations, *Powder Technology: Powder Technol.* **279**, 2015, 49–60, <https://doi.org/10.1016/j.powtec.2015.03.038>.
- [6] B. Mamen, J. Song, T. Barriere and J.-C. Gelin, Experimental and numerical analysis of the particle size effect on the densification behaviour of metal injection moulded tungsten parts during sintering, *Powder Technol.* **270** (Part A), 2015, 230–243, <https://doi.org/10.1016/j.powtec.2014.10.019>.
- [7] A. Royer, T. Barrière and J.-C. Gelin, Development and Characterization of a Metal Injection Moulding Based Sourced Inconel 718 Feedstock Based on Polyhydroxyalkanoates, *Metals* **6**, 2016, 89, <https://doi.org/10.3390/met6040089>.
- [8] A. Royer, T. Barriere and J.C. Gelin, The degradation of poly(ethylene glycol) in an Inconel 718 feedstock in the metal injection moulding process, *Powder Technology: Powder Technol.* **284**, 2015, 467–474, <https://doi.org/10.1016/j.powtec.2015.07.032>.
- [9] A. Royer, T. Barrière, J.-C. Gelin and L. Hilliou, Development and characterisation of a biosourced feedstock of super-alloy in metal injection moulding process, *Powder Metall.* 2017 <http://www.tandfonline.com/eprint/79KxA3pha8fhPdVtkYJ7/full>, Accessed 20 March 2017.
- [10] S. Thomas, Y. Grohens and P. Jyotishkumar, *Characterization of Polymer Blends: Miscibility, Morphology and Interfaces*, 2014, John Wiley & Sons.
- [11] M. Sheth, R.A. Kumar, V. Davé, R.A. Gross and S.P. McCarthy, Biodegradable polymer blends of poly(lactic acid) and poly(ethylene glycol), *J. Appl. Polym. Sci.* **66**, 1997, 1495–1505, [https://doi.org/10.1002/\(SICI\)1097-4628\(19971121\)66:8<1495::AID-APP10>3.0.CO;2-3](https://doi.org/10.1002/(SICI)1097-4628(19971121)66:8<1495::AID-APP10>3.0.CO;2-3).
- [12] R.V. Castillo and A.J. Müller, Crystallization and morphology of biodegradable or biostable single and double crystalline block copolymers, *Progress in Polymer Science: Prog. Polym. Sci.* **34**, 2009, 516–560, <https://doi.org/10.1016/j.progpolymsci.2009.03.002>.
- [13] S. Ebnesaajad, *Handbook of Biopolymers and Biodegradable Plastics: Properties, Processing and Applications*, 2013, William Andrew.
- [14] S.T. Lin and R.M. German, Interaction between binder and powder in injection moulding of alumina, *J. Mater. Sci. J. Mater. Sci.* **29**, 1994, 5207–5212, <https://doi.org/10.1007/BF01151118>.
- [15] T. Chartier, M. Ferrato and J.F. Baumard, Supercritical Debinding of Injection Moulded Ceramics, *Journal of the American Ceramic Society. J. Am. Ceram. Soc.* **78**, 1995, 1787–1792, <https://doi.org/10.1111/j.1151-2916.1995.tb08890.x>.
- [16] T. Shimizu, Y. Murakoshi, K. Wechitayakhlung, T. Sano and H. Negishi, Characterization of the molding methods and the binder system in the MIM process, *Journal of Materials Processing Technology. J. Mater. Process. Technol.* **63**, 1997, 753–758, [https://doi.org/10.1016/S0924-0136\(96\)02718-5](https://doi.org/10.1016/S0924-0136(96)02718-5).
- [17] T. Chartier, F. Bordet, E. Delhomme and J. François Baumard, Extraction of binders from green ceramic bodies by supercritical fluid: influence of the porosity, *Journal of the European Ceramic Society. J. Eur. Ceram. Soc.* **22**, 2002, 1403–1409, [https://doi.org/10.1016/S0955-2219\(01\)00474-5](https://doi.org/10.1016/S0955-2219(01)00474-5).
- [18] R. Zhao, X.J. Li, M. Wan, J.Q. Han, B. Meng and Z.Y. Cai, Fracture behavior of Inconel 718 sheet in thermal-aided deformation considering grain size effect and strain rate influence, *Materials & Design. Mater. Des.* **130**, 2017, 413–425, <https://doi.org/10.1016/j.matdes.2017.05.089>.
- [19] Ö. Özgün, H. Özkan Gülsoy, R. Yılmaz and F. Findik, Injection molding of nickel based 625 super-alloy: Sintering, heat treatment, microstructure and mechanical properties, *Journal of Alloys and Compounds. J. Alloys Compd.* **546**, 2013, 192–207, <https://doi.org/10.1016/j.jallcom.2012.08.069>.
- [20] Ö. Özgün, H.Ö. Gülsoy, R. Yılmaz and F. Findik, Microstructural and mechanical characterization of injection molded 718 super-alloy powders, *Journal of Alloys and Compounds. J. Alloys Compd.* **576**, 2013, 140–153, <https://doi.org/10.1016/j.jallcom.2013.04.042>.
- [21] K.D. Ramkumar, W.S. Abraham, V. Vijayash, N. Arivazhagan and A.M. Rabel, Investigations on the microstructure, tensile strength and high temperature corrosion behaviour of Inconel 625 and Inconel 718 dissimilar joints, *J. Manuf. Process.* 2017, 306–322, Complete <https://doi.org/10.1016/j.jmapro.2016.12.018>.
- [22] R. Cozar and A. Pineau, Morphology of γ_1 and γ_2 precipitates and thermal stability of inconel 718 type alloys, *MT* **4**, 1973, 47–59, <https://doi.org/10.1007/BF02649604>.
- [23] J.H. (Dept of M.S. and He, T. University, Beijing, 100084, C.F. and K.Y. (Chugoku N.I.R. Institute, H. 2-2-2, Kure, Hiroshima, 737-01, J. (To whom correspondence should be Address, γ' Precipitate in Inconel 718, 10 (2009) 293–303.

- [24] S. Chen, M. Zhao and L. Rong, Role of v_2 characteristic on the hydrogen embrittlement susceptibility of Fe–Ni–Cr alloys, *Corrosion-Science-Corros. Sci.* **101**, 2015, 75–83, <https://doi.org/10.1016/j.corsci.2015.09.003>.
- [25] Valencia, McCabe, Hens, Hansen and Bose, Microstructure and Mechanical Properties of Inconel 625 and 718 Alloys Processed by Powder Injection Molding, *Super-alloys 718, 625, 706 and Various Derivatives*, 1994, 934–945.
- [26] C. Quinard, T. Barriere and J.C. Gelin, Development and property identification of 316L stainless steel feedstock for PIM and μ PIM, *Powder-Technology-Powder Technol.* **190**, 2009, 123–128, <https://doi.org/10.1016/j.powtec.2008.04.044>.
- [27] G. Chen, P. Cao, G. Wen and N. Edmonds, Debinding behaviour of a water soluble PEG/PMMA binder for Ti metal injection moulding, *Materials-Chemistry-and-Physics-Mater. Chem. Phys.* **139**, 2013, 557–565, <https://doi.org/10.1016/j.matchemphys.2013.01.057>.
- [28] J. Hidalgo, A. Jiménez-Morales, T. Barriere, J.C. Gelin and J.M. Torralba, Capillary rheology studies of INVAR 36 feedstocks for powder injection moulding, *Powder-Technology-Powder Technol.* **273**, 2015, 1–7, <https://doi.org/10.1016/j.powtec.2014.12.027>.
- [29] D. Zhou, J. Shao, G. Li, J. Sun, X. Bian and X. Chen, Crystallization behavior of PEG/PLLA block copolymers: Effect of the different architectures and molecular weights, *Polymer-Polymer* **62**, 2015, 70–76, <https://doi.org/10.1016/j.polymer.2015.02.019>.
- [30] A. Oradei-Basile and J.F. Radavich, A current TTT diagram for wrought alloy 718, *Super-Alloys 718*, 1991, 325–335.
- [31] J.M. Oblak, D.F. Paulonis and D.S. Duvall, Coherency strengthening in Ni base alloys hardened by DO22 v_2 precipitates, *MT 5*, 1974, 143, <https://doi.org/10.1007/BF02642938>.
- [32] H. Feldstein and O. Mendoza, Analysis and Elimination of Time Dependent Notch Sensitivity in Alloy 718, *Super-Alloys 1989*, 655–671.
- [33] R.C. Reed, K.A. Green, P. Caron, T.P. Gabb, M.G. Fahrman, E.S. Huron and S.A. Woodard, The Effect of Carbide Morphologies on Elevated Temperature Tensile and Fatigue Behavior of a Modified Single Crystal Ni-Base Super-alloy, http://www.tms.org/Super-alloys/10.7449/2008/Super-alloys_2008_489_497.pdf, 2018, Accessed 15 June 2017.
- [34] J.W. Brooks and P.J. Bridges, Metallurgical Stability of Inconel Alloy 718, *Super-Alloys 1988*, 33–42.

Graphical abstract



alt-text: Unlabelled Image

Highlights

- New metal injection-moulding feedstock made with bio-sourced polymers and Inconel 718;
- Supercritical CO₂ as solvent applied to high-loaded feedstock;
- Optimal parameters with innovative supercritical CO₂ debinding method;
- Better mechanical properties after supercritical debinding and heat treatment;

Queries and Answers

Query:

Your article is registered as a regular item and is being processed for inclusion in a regular issue of the journal. If this is NOT correct and your article belongs to a Special Issue/Collection please contact s.palaniswamy@elsevier.com immediately prior to returning your corrections.

Answer: Yes

Query:

Please confirm that given names and surnames have been identified correctly and are presented in the desired order, and please carefully verify the spelling of all authors' names.

Answer: Yes

Query:

The author names have been tagged as given names and surnames (surnames are highlighted in teal color). Please confirm if they have been identified correctly.

Answer: Yes

Query:

The country name "France" has been inserted for all affiliations field. Please check and confirm if correct.

Answer:

Query:

Please check the hierarchy of the section headings and confirm if correct.

Answer: Yes

Query:

Please provide the corresponding grant number(s) for the following grant sponsor(s): "FUI ProPIM".

Answer: sorry, with have no grant number

Query:

Please provide the volume number and page range for the bibliography in Ref. [9].

Answer: